Experimental verification of a bridge-shaped, nonlinear vibration energy harvester

Citation: Gafforelli, Giacomo, Alberto Corigliano, Ruize Xu, and Sang-Gook Kim. "Experimental Verification of a Bridge-Shaped, Nonlinear Vibration Energy Harvester." Applied Physics Letters 105, no. 20 (November 17, 2014): 203901. © 2014 AIP Publishing LLC

As Published: http://dx.doi.org/10.1063/1.4902116

Publisher: American Institute of Physics (AIP)

Persistent URL: http://hdl.handle.net/1721.1/98506

Version: Final published version: final published article, as it appeared in a journal, conference proceedings, or other formally published context

AIP | Applied Physics Letters

Experimental verification of a bridge-shaped, nonlinear vibration energy harvester

Giacomo Gafforelli, Alberto Corigliano, Ruize Xu, and Sang-Gook Kim

Citation: Applied Physics Letters **105**, 203901 (2014); doi: 10.1063/1.4902116
View online: http://dx.doi.org/10.1063/1.4902116
View Table of Contents: http://scitation.aip.org/content/aip/journal/apl/105/20?ver=pdfcov
Published by the AIP Publishing

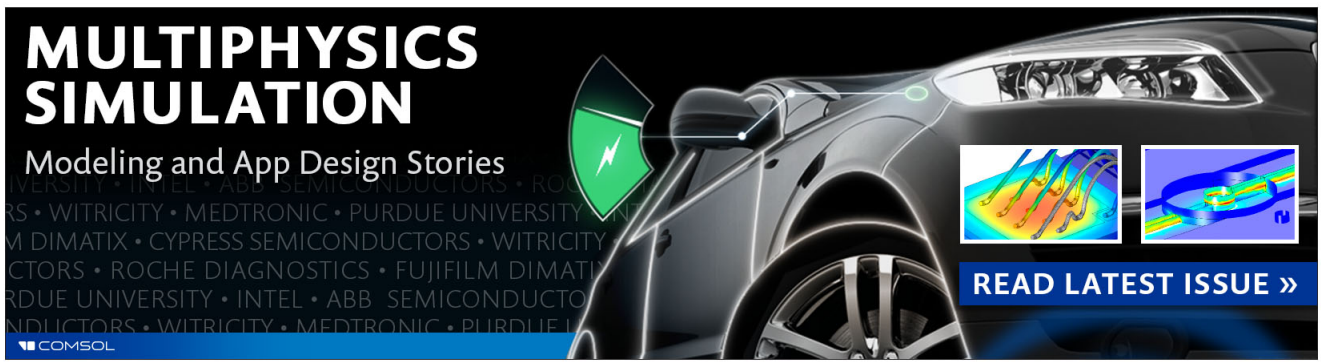

Experimental verification of a bridge-shaped, nonlinear vibration energy harvester

Giacomo Gafforelli,[1,a)] Alberto Corigliano,[1] Ruize Xu,[2] and Sang-Gook Kim[2]
[1]*Department of Civil and Environmental Engineering, Politecnico di Milano, Milano, 20133, Italy*
[2]*Department of Mechanical Engineering, Massachusetts Institute of Technology, Cambridge, Massachusetts 02139, USA*

(Received 4 September 2014; accepted 7 November 2014; published online 18 November 2014)

This paper reports a comprehensive modeling and experimental characterization of a bridge shaped nonlinear energy harvester. A doubly clamped beam at large deflection requires stretching strain in addition to the bending strain to be geometrically compatible, which stiffens the beam as the beam deflects and transforms the dynamics to a nonlinear regime. The Duffing mode non-linear resonance widens the frequency bandwidth significantly at higher frequencies than the linear resonant frequency. The modeling includes a nonlinear measure of strain coupled with piezoelectric constitutive equations which end up in nonlinear coupling terms in the equations of motion. The main result supports that the power generation is bounded by the mechanical damping for both linear and nonlinear harvesters. Modeling also shows the power generation is over a wider bandwidth in the nonlinear case. A prototype is manufactured and tested to measure the power generation at different load resistances and acceleration amplitudes. The prototype shows a nonlinear behavior with well-matched experimental data to the modeling.
[http://dx.doi.org/10.1063/1.4902116]

Due to intrinsic limitations of linear resonance-based energy harvesters in converting vibration to electrical energy such as high resonant frequencies and small bandwidths,[1] many researchers focused their attention to nonlinear resonant mechanisms with the aim to increase the overall performance of such devices. Two major nonlinear mechanisms have been proposed: bistable beams[2] and monostable hardening/softening structures.[3,4] In this paper, we focus on nonlinear monostable hardening structures where stretching strains are induced in a doubly clamped bridge-shaped piezoelectric beam with a concentrated mass in the middle. The doubly clamped beam at large deflection requires stretching strain in addition to the bending strain to be geometrically compatible, which stiffens the beam as the beam deflects, transforms the dynamics to the nonlinear regime, and results in a hardening Duffing oscillator. Hajati and Kim[5] have shown the effectiveness of a micro-machined *Ultrawide bandwidth energy harvester* (UWBEH) with a high power density and a very wide bandwidth. The results provided by that work was modeled with simple nonlinear lumped system. Gafforelli *et al*. recently proposed a first complete theoretical modeling of the hardening mechanism.[6] A detailed modeling accounting for the actual piezoelectric contribution to the oscillator has been developed. The sectional behavior of the bridge-beam has been studied through the Classical Lamination Theory (CLT) specifically modified to introduce the piezoelectric coupling and nonlinear Green-Lagrange strain tensor. A final lumped parameter model has been built through Rayleigh-Ritz method resulting in coupled motion equations, which include additional non-common terms originating from a correct analysis of piezoelectrics coupling in nonlinear strain context. The motion equations can be obtained using Euler Lagrange approach

$$\frac{\mathrm{d}}{\mathrm{d}t}\frac{\partial \mathcal{K}}{\partial \dot{q}_i} + \frac{\partial \mathcal{E}}{\partial q_i} - \frac{\partial \mathcal{W}}{\partial q_i} + \frac{\partial \mathcal{D}}{\partial \dot{q}_i} = 0, \tag{1}$$

where $\mathcal{K}$, $\mathcal{E}$, $\mathcal{W}$, and $\mathcal{D}$ are the kinetic and internal energy, the external work, and the dissipation function; q_i represents the variables of the system: the vertical displacement of the mass (w) and the voltage across piezoelectric electrodes (v). The computation of Eq. (1) leads to the equation of motions (see Ref. Gafforelli *et al*.[6])

$$\begin{aligned} &m\ddot{w} + c_M\dot{w} + k_L w + k_N w^3 + \Theta_N v w = -m\ddot{y}_{ext} \\ &C_0 v - 1/2\,\Theta_N w^2 = q \quad \text{and} \quad \dot{q} = R^{-1}v. \end{aligned} \tag{2}$$

In Eq. (2), m is the total mass, c_M is the mechanical damping coefficient, k_L and k_N are the linear, which includes bending and residual stresses, and nonlinear stiffnesses, Θ_N is the global piezoelectric coupling coefficient, C_0 is the total capacitance, and R is the equivalent load resistance of the circuitry required for the power management.

Nonlinear piezoelectric coupling terms are obtained in Eq. (2) because the internal energy of the beam includes a coupled energy ($\mathcal{E}_{ME}$) which is nonlinear since the piezoelectric stress (proportional to the voltage) multiplies the Green-Lagrangian strain (quadratic to the displacement)

$$\mathcal{E}_{ME} = 1/2\,\Theta_N v w^2. \tag{3}$$

Thus, in applying Euler-Lagrange equations when performing the derivation of $\mathcal{E}$ with respect to w and v, the computation ends up in nonlinear coupling terms.

Eq. (2) is studied through *Harmonic Balance Method* (HBM) in order to highlight the influence of piezoelectric

a)Electronic mail: giacomo.gafforelli@polimi.it

coupling on both stiffness and damping; oscillation amplitude, voltage, and power responses have been computed in the mechanical and electrical frequency domain. The contribution of an external load resistance to the harvester performance has been discussed showing that the injected electrical damping c_E (Eq. (4)) depends on the amplitude of the displacement and on the value of load resistance. It also has a maximum for a specific value defined by system parameters

$$c_E = \omega_0 m \frac{\kappa_{\eta v}^2 \Omega_E}{4\left(4\Omega_M^2 + \Omega_E^2\right)} Y^2, \tag{4}$$

where $Y = W/W_0$ is the oscillation amplitude normalized with respect to the linear static displacement $W_0 = -m|\ddot{y}_{ext}|/k_L$ and $\kappa_{\eta v} = W_0\Theta_N/\sqrt{k_L C_0}$ is the effective nonlinear piezoelectric coupling coefficient. The model shows that the power generation envelope has two peaks that occur when the induced electrical damping matches the mechanical damping of the system as it happens for linear resonant harvesters (Figure 1). Thus, similar to linear resonators, the maximum power of the nonlinear harvester is bounded by the mechanical damping. However, it has a much wider bandwidth.

A mesoscale harvester has been fabricated to perform an experimental validation of the modeling (Figure 2). The device is composed of a structural support, a bridge-shaped piezoelectric beam, and a lead concentrated mass. The beam consists of a 0.3 mm thick Macro Fiber Composite piezoelectric patch (MFC M8514-P1) glued on a 0.06 mm thick aluminum layer with an epossidic glue. Such a thickness of the aluminum layer has been chosen in order to reduce the bending strain and widen the nonlinear regime of the beam. Moreover, the amount of active material is much more than the non-active resulting in higher piezoelectric coupling. The beam has been clamped to the support structure through pressure and friction and the lead tip mass has been glued at the center of the beam. Small aluminum plates have been interposed between the beam and the support and between

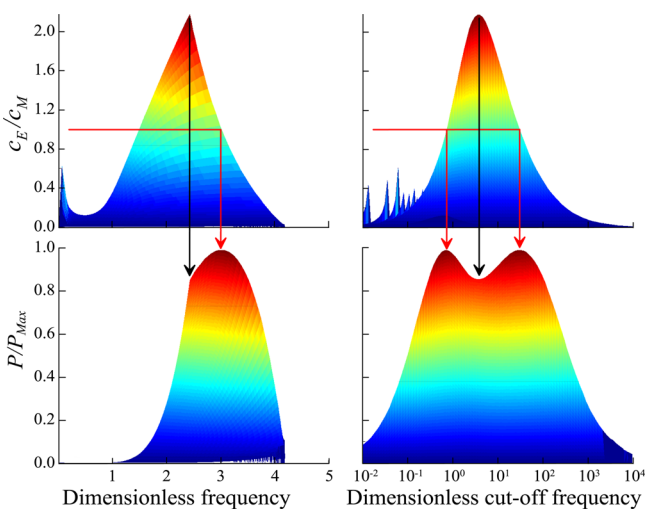

FIG. 1. Normalized electrical damping and power generation vs. dimensionless excitation frequency, $\Omega_M = \omega\omega_0^{-1}$ and cut-off frequency, $\Omega_E = (RC_0\omega_0)^{-1}$. Where ω is the excitation frequency and ω_0 is the resonance frequency. The peak power generation is obtained when electrical and mechanical damping matches.

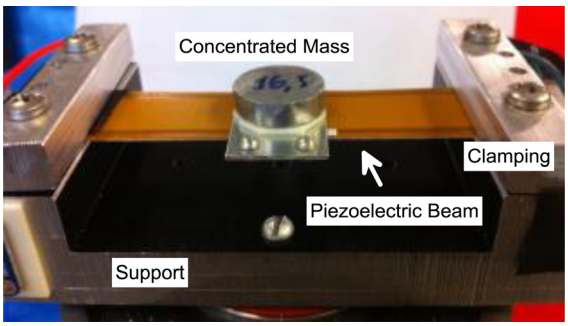

FIG. 2. Mesoscale prototype of the double-clamped piezoelectric beam.

the beam and the clamps to avoid cracks. The clamping is realized such that any pre-shape is avoided, e.g., arc shape or tilted shape, in order to prevent unstable phenomena that can affect the pure hardening behavior. The whole system has been excited by a Labworks electromagnetic shaker type ET126B-1, which is controlled by Prema ARB 1000 signal generator controlled in a built-up close loop system that controls the acceleration and the frequency of the shaker through an accelerometer. The MFC patch has been connected to an external variable resistance and the voltage signal has been fed into a FFT analyzer. The beam of the final prototype has an overall length of 76.2 mm (3 in.), which includes a central concentrated mass of 16.5 g that occupies 10 mm. The width of the beam is 20 mm which is the width of the MFC (the active piezoelectrics is only 14 mm). The aluminum layer width and thickness has been chosen to assure torsional stiffness and to avoid tilting induced by non-perfect symmetry of the mass or other uncertainties such as non-alignment of the beam. This has been also obtained using lead as material for the concentrated mass, thus assuring the necessary high weight in order to induce strong non-linearity, in a compact volume. First, we have characterized the MFC patch. It consists of rectangular piezoelectric fibers sandwiched between interdigitated electrodes and polyimide films. The measured total capacitance was 4 nF, while the piezoelectric strain coefficients were: $d_{31} = -90.63$ pm/V and $d_{33} = 206.44$ pm/V. These values which refer to the whole patch are lower than the one reported in the MFC datasheet (www.smart-material.com), but is not clear if the online data refer to the sole piezoelectric fibers or to the whole MFC. The prototype has been tested in open circuit in order to estimate the overall mechanical quality factor $Q_M = \omega_0 m/c_M$. Different values of input acceleration (0.3 g, 0.4 g, and 0.5 g) have been used and fitted using Q_M as fitting parameter. First, as it can be seen from Figure 3, the model qualitatively and quantitatively reproduces the experimental measurements for estimated quality factor in the range of 10–11. The value of Q_M is low compared to other systems in the literature and is basically due to energy loss in the end clamps, damping in the epoxy and polymer layers of the MFC, and also due to the bonding to the aluminum layer. The second observation is that the model matches the measurements only in the resonance regime, while at low and high frequencies the voltage data are significantly higher than the experimental ones. To explain this, one should notice that the measured voltage signal in the resonance regime has double the frequency than the excitation while this is not happening when the oscillation amplitude is lower and the input and output frequency

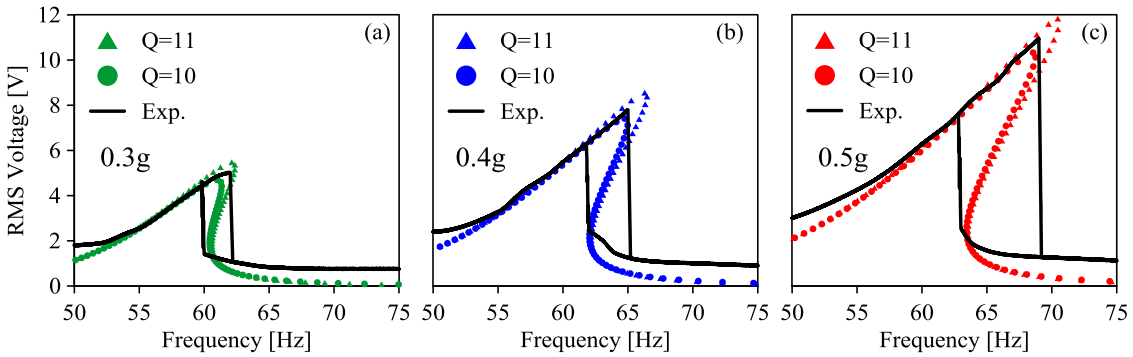

FIG. 3. Open circuit response at 0.3 g (a), 0.4 g (b), and 0.5 g (c) input accelerations. Experimental measured data (solid line) are fitted with the modeling for mechanical quality factor equal to 10 (dot) and 11 (triangle).

perfectly match (Figure 4). As the stretching mode has double frequency than the bending one, it is clear that the low amplitude signal originates from bending strain while at high amplitudes, where the nonlinear strain dominates, the voltage is generated by the stretching. However, for symmetry reasons the global voltage due to bending should be null. The model accounts for perfect geometry, thus, the bending coupling is completely neglected. On the other hand, the real device geometry is far from being perfect and a residual asymmetry persists. For this reason, when bending dominates over stretching the device imperfections are more evident and the model fails in depicting the experimental data. Once calibrated, the model has been used to predict the response of the prototype coupled to external resistive loads, the tests have been performed for 0.3, 0.4, and 0.5 g input acceleration and good accordance between measurements and predictions (employing $Q_M = 10.3$) has been obtained. Figure 5 collects the resulting power generation in case of 0.5 g acceleration. As it can be seen from Figure 5, the value of jump-down frequency, which roughly speaking is the frequency where the oscillation amplitude is at maximum, is slightly modified by the load resistance. This phenomenon had been already introduced by Ref. 7 for linear harvesters and had been extended to nonlinear systems by Ref. 6. The coupling with piezoelectrics connected to a resistive load acts as an additional stiffness (thus modifying the resonance frequency and distinguishing between open and short circuit responses) and clearly as a source of damping. By tuning the external resistance one can control the electrical

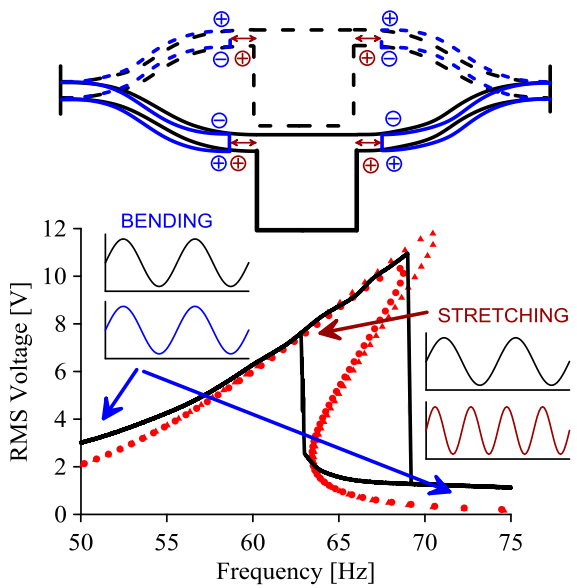

FIG. 4. At low oscillation amplitudes, the input and output voltage have the same frequency because bending mode is activated, while at high oscillation amplitudes, stretching mode is activated and the output signal has double frequency than the input.

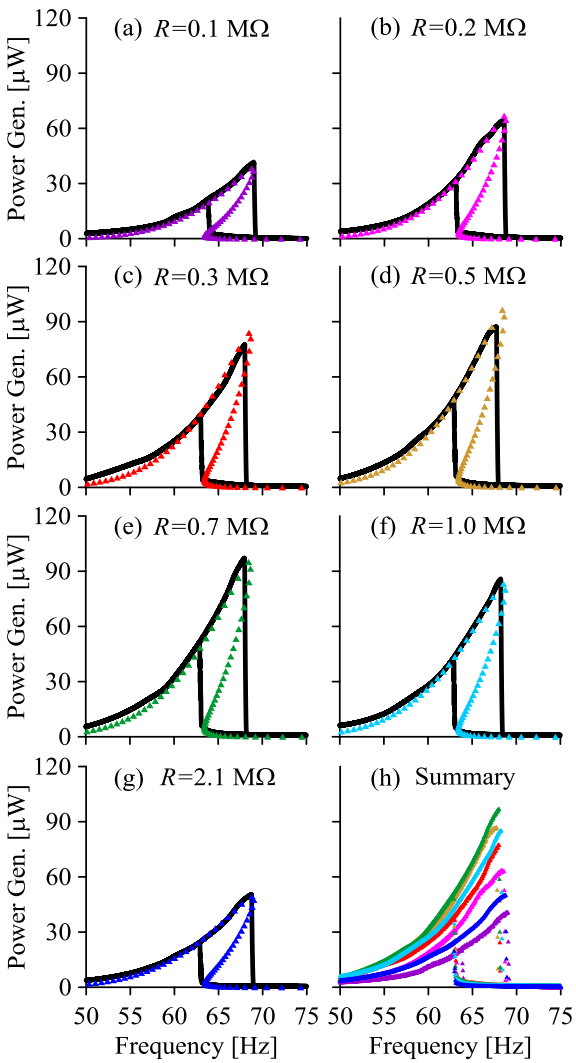

FIG. 5. Comparison of theoretical (triangle) and measured (solid line) power generation at 0.5 g acceleration and load resistance equal to (a) 0.1 MΩ, (b) 0.2 MΩ, (c) 0.3 MΩ, (d) 0.5 MΩ, (e) 0.7 MΩ, (f) 1.0 MΩ, (g) 2.1 MΩ, and (h) summary of experimental data.

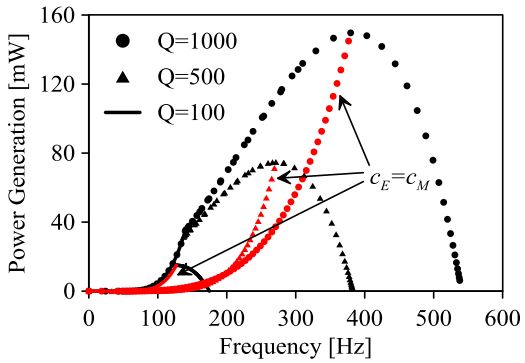

FIG. 6. Theoretical performances of the prototype for different mechanical damping values.

damping injected in the system and since the jump-down frequency strongly depends on the damping[8] the bandwidth of the response is modified. Moreover, load resistance and electrical damping does not depend linearly, indeed while moving from high towards low resistances the jump-down frequency first reduces and then increases. There exists a value of load resistance, where the injected damping is maximum depending on materials and geometrical parameters. Consequently, it cannot be arbitrarily increased. In the studied case, the mechanical damping is much higher than the electrically induced one and the jump-down variation is little emphasized. This observation is extremely important in order to understand the role played by the mechanical damping in nonlinear monostable energy harvesters. Low mechanical damping is required not only to maximize the output but also to exploit the maximum bandwidth amplification. However, the electrical damping should not be augmented indefinitely but should be controlled in order to avoid the jump down phenomenon such that the oscillation amplitude will always stay in the high energy branch (resonant branch) of the frequency response. Accordingly to this, the theoretical performances of the prototype are reported in Figure 6 for different values of mechanical quality factor. In particular, the bandwidth can be increased from 7 Hz up to 400 Hz and the power generation from barely 0.2 mW up to 150 mW.

In summary, this paper has proposed an experimental validation of a theoretical model of a bridge-shaped nonlinear vibration energy harvester. The model includes nonlinear coupling terms with piezoelectrics, and it shows good accordance with experimental data for different load resistances and acceleration inputs. Further experiments should be performed with low damping in order to demonstrate the real potentiality of the prototype in terms of increased frequency bandwidth and power generation. In particular, future tests will be focused on showing that the maximum power is obtained when the electrical induced damping matches the mechanical damping as predicted by the modeling.

Giacomo Gafforelli thanks Professor Sang-Gook Kim and the Micro and Nano Systems Laboratory for being hosted as visiting Student at MIT. Giacomo Gafforelli and Alberto Corigliano thank The Fondazione Rocca, Progetto Rocca GSF, and Eniac joint undertaking, project Lab4MEMS, Grant No. 325622, for partial funding this research.

[1]Y. B. Jeon, R. Sood, J.-H. Jeong, and S.-G. Kim, Sens. Actuators, A **122**, 16 (2005).
[2]R. L. Harne and K. W. Wang, Smart Mater. Struct. **22**, 023001 (2013).
[3]B. P. Mann, D. A. Barton, and B. A. Owens, J. Intell. Mater. Syst. Struct. **23**, 1451 (2012).
[4]M. F. Daqaq, R. Masana, A. Erturk, and D. Dane Quinn, Appl. Mech. Rev. **66**, 040801 (2014).
[5]A. Hajati and S.-G. Kim, Appl. Phys. Lett. **99**, 083105 (2011).
[6]G. Gafforelli, R. Xu, A. Corigliano, and S.-G. Kim, Energy Harvesting Syst. (published online July 2014).
[7]N. E. Du Toit, B. L. Wardle, and S.-G. Kim, Integr. Ferroelectr. **71**, 121 (2005).
[8]M. Brennan, I. Kovacic, A. Carrella, and T. Waters, J. Sound Vib. **318**, 1250 (2008).